

## Article

# Crystal Structure of Mixed Np(V)-Ammonium Carbonate

Iurii M. Nevolin <sup>1,2</sup>, Vladimir G. Petrov <sup>2,\*</sup> , Mikhail S. Grigoriev <sup>1</sup> , Alexei A. Averin <sup>1</sup> ,  
Andrey A. Shiryaev <sup>1</sup> , Anna D. Krot <sup>2</sup> , Konstantin I. Maslakov <sup>2</sup> , Yury A. Teterin <sup>2,3</sup>  
and Alexander M. Fedoseev <sup>1</sup>

<sup>1</sup> Frumkin Institute of Physical Chemistry and Electrochemistry, Russian Academy of Sciences, Leninsky Prospect 31 bld. 4, 119071 Moscow, Russia

<sup>2</sup> Department of Chemistry, Lomonosov Moscow State University, Leninskie Gory 1 bld. 3, 119991 Moscow, Russia

<sup>3</sup> National Research Center “Kurchatov Institute”, pl. Akademika Kurchatova, 1, 123182 Moscow, Russia

\* Correspondence: vladimir.g.petrov@gmail.com

**Abstract:** This work presents details of the synthesis, properties and structure of a novel neptunium carbonate  $(\text{NH}_4)[\text{NpO}_2\text{CO}_3]$ , a member of the  $\text{M}[\text{AnO}_2\text{CO}_3]$  ( $\text{M} = \text{K}, (\text{NH}_4), \text{Rb}, \text{Cs}$ ) class of compounds. Carbonates play an important role in the migration of actinides in the environment, and thus are relevant for handling and disposal of radioactive wastes, including spent nuclear fuel and vitrified raffinates. Knowledge of the crystallographic structure of these compounds is important for models of the environmental migration behavior based on thermodynamic descriptions of such chemical processes.  $(\text{NH}_4)[\text{NpO}_2\text{CO}_3]$  crystals were obtained during long-term hydrothermal treatment of Np(VI) in aqueous ammonia at 250 °C. X-ray diffraction (XRD) and X-ray photoelectron spectroscopy (XPS) show that a single-phase sample containing only Np(V) was obtained. Structural features of  $(\text{NH}_4)[\text{NpO}_2\text{CO}_3]$  were elucidated from single crystal X-ray diffraction and confirmed by vibrational spectroscopy. The results obtained are of interest both for fundamental radiochemistry and for applied problems of the nuclear fuel cycle.

**Keywords:** neptunium; carbonates; structural investigations; ammonia; hydrothermal synthesis



**Citation:** Nevolin, I.M.; Petrov, V.G.; Grigoriev, M.S.; Averin, A.A.; Shiryaev, A.A.; Krot, A.D.; Maslakov, K.I.; Teterin, Y.A.; Fedoseev, A.M. Crystal Structure of Mixed Np(V)-Ammonium Carbonate. *Symmetry* **2022**, *14*, 2634. <https://doi.org/10.3390/sym14122634>

Academic Editors: Balaraman Kaluvu and Eshani Hettiarachchi

Received: 30 October 2022

Accepted: 8 December 2022

Published: 13 December 2022

**Publisher's Note:** MDPI stays neutral with regard to jurisdictional claims in published maps and institutional affiliations.



**Copyright:** © 2022 by the authors. Licensee MDPI, Basel, Switzerland. This article is an open access article distributed under the terms and conditions of the Creative Commons Attribution (CC BY) license (<https://creativecommons.org/licenses/by/4.0/>).

## 1. Introduction

Predicting the behavior of radioactive wastes containing such radiotoxic and long-lived actinides as neptunium or plutonium is the basis of safety at the final stages of the nuclear fuel cycle [1]. Modeling the behavior of actinides in the environment, based on the thermodynamic description of the processes of sorption, dissolution, etc., are among the most powerful predictive tools [2–4]. Implementation of this approach requires knowledge of the basic thermodynamic ( $\Delta H_f^\circ$ ,  $\Delta S^\circ$ ) constants characterizing individual actinide phases. These values can be obtained experimentally from studies of single-phase samples, or calculated from known crystal structures of the compounds using quantum chemistry approaches [5]. An alternative approach is the use of non-radioactive chemically similar elements; however, the validity of extrapolation of the results in this case is limited [6,7]. Thus, synthesis and structural description of actinide phases, which may form during radioactive waste management, is an important step in creating predictive models. Carbonate anions and alkali metal cations are integral components of natural media [8], while ammonium cations play an important role in a number of nuclear fuel cycle processes [9]. This combination explains the urgency in the identification of new compounds in the  $\text{An-CO}_3\text{-H}_2\text{O-M}$  ( $\text{M}: \text{NH}_4, \text{K}, \text{Na}$ ) system.

Double carbonates of pentavalent actinides and alkali metals/ammonium have been the subject of research since the 1960s [10–12]. From a technological point of view, this is explained by the unique properties of pentavalent actinides, namely, the very low solubility of their carbonate complexes with the outer-sphere cations listed above, compared to carbonate complexes of f-elements in oxidation states +3, +4 and +6, which, for example, can

be used for separation and purification of americium and curium [13]. In addition, double carbonates of pentavalent actinides are widely used as starting compounds for the synthesis of compounds with these valence forms, in particular Pu(V). Interest in these compounds is also related to the high stability of Np(V) under environmental conditions [14,15]. Therefore, these carbonate complexes are studied by various physicochemical methods, see, for example, recent studies of the individual complexation of Np(V) [16] and U(V), U(VI) [17], as well as in their mixture [18] in carbonate solutions in a wide range of experimental conditions by electrochemical and spectroscopic methods. It is thus unexpected that the crystal structure of many widely occurring Np(V) complexes has not been completely solved until recently. Only models obtained from powder diffraction patterns are known [10,11]. This can be explained by the fact that double carbonates of pentavalent actinides and alkali metals precipitate as extremely fine crystalline powders that do not recrystallize even under hydrothermal conditions. In this work, we found a synthetic approach that allows one to obtain  $(\text{NH}_4)[\text{NpO}_2\text{CO}_3]$  crystals suitable for single crystal X-ray diffraction and refine the structure of this compound.

## 2. Materials and Methods

### 2.1. Synthesis of $(\text{NH}_4)[\text{NpO}_2\text{CO}_3]$ Crystals

*Caution!*  $^{237}\text{Np}$  is radioactive and dangerous. Therefore, precautions and radiation protection are required for the experiments. All described operations with radioactive materials were carried out in accordance with laws of Russian Federation.

Nitric, perchloric acids and ammonia aqueous solution were the reagent grade.  $^{237}\text{Np}$  in the form of  $\text{NpO}_2$  was purchased from Rosatom State Corporation. According to alpha spectrometry, the radiochemical purity of the substance was higher than 99.9%;  $^{239}\text{Pu}$  was the only observable impurity. Neptunium stock solution was obtained by dissolving solid Np(IV) oxalate in 16 mol/L  $\text{HNO}_3$  upon heating. Np valence state in all the solutions was controlled by spectrophotometry—the concentration of Np(V) in all cases was less than 0.2 mass. %. All operations were carried out in an air atmosphere, which was the main source of  $\text{CO}_2$  during the synthesis.

The basis of the synthesis was hydrothermal treatment of the Np(VI) in the presence of ammonia solution. To oxidize all neptunium to Np(VI), aliquots of the neptunium stock solution (0.5 mL of 0.04 mmol solution) were evaporated with concentrated perchloric acid; solid residues were dissolved in water and then precipitated by adding ammonium. The precipitates were rinsed with water and dispersed in ~0.3 mL of ammonia aqueous solution with 1.3 mol/L and 13 mol/L concentration. The dispersions were transferred in PTFE test tubes with screw caps and placed in glass ampoules with ~0.5 mL of ammonia aqueous solution (Figure S1). The glass ampoules were sealed with a gas burner and placed in oven at 250 °C for up to 45 days.

### 2.2. X-ray Structural Analysis

Single crystal X-ray diffraction experiment was carried out using four-circle diffractometer KAPPA APEX II (Bruker AXS, Billerica, MA, USA;  $\text{MoK}\alpha$  radiation) equipped with a 2D detector. The unit cell constants were refined over the whole dataset. Experimental intensities were corrected for absorption using the SADABS program [19]. The structures were solved by direct method (SHELXS97 [20]) and refined using the full-matrix least-squares method (SHELXL-2018/3 [21]) on  $F^2$  in anisotropic approximation for all non-hydrogen atoms. Hydrogen atoms were located from a difference Fourier synthesis and refined with restraints (equal  $U_{\text{iso}}(\text{H})$ , equal N-H and H...H distances).

Powder X-ray diffraction (PXRD) measurements were performed using Aeris X-ray diffractometer (Malvern Panalytical, Almelo, The Netherlands) with  $\text{CuK}\alpha$  radiation and PIXcel3D detector. Diffraction patterns were recorded with  $2\theta = 0.011^\circ$  step in Bragg–Brentano geometry. Single crystals of  $(\text{NH}_4)[\text{NpO}_2\text{CO}_3]$  were milled in a glove box and measured on a zero-background silicon holder. The lattice parameters were refined from the powder XRD patterns by Le Bail method [22] using Jana2006 software [23].

### 2.3. X-ray Photoelectron Spectroscopy

X-ray photoelectron spectroscopy (XPS) was carried out according to the generally accepted method. Spectra were obtained using Axis Ultra DLD spectrometer (Kratos Analytical, Manchester, UK). Monochromatic Al K $\alpha$  radiation with  $h\nu = 1486.6$  eV and power of 150 W was used. The analyzer transmission energies were 160 eV for the overall spectrum and 40 eV for scans with high energy resolution. Double sided conductive tape was used for sample mounting. C1s peak at a binding energy of 285.0 eV was used for energy calibration, excess charge was neutralized by Kratos system.

### 2.4. Vibrational Spectroscopy

Vibrational spectroscopy details were previously described in [24]. inVia Relfex spectrometer (Renishaw, Wotton-under-Edge, UK) was used to obtain Raman spectra. Spectra acquisition was performed using Peltier-cooled CCD detector, laser with the wavelength of 532 nm and 100 $\times$  objective with NA of 0.8. LaserCheck device (Coherent, Santa Clara, CA, USA) was used to control laser power that does not exceed 0.2 mW. Silicon sample and high-quality CVD diamond were used as standards for wavenumber calibration. Laser spot size varied from 2 to 5  $\mu\text{m}$ .

Infra-red (IR) spectroscopy was carried out using FTIR SpectrumOne spectrometer (PerkinElmer, Waltham, MA, USA) equipped with an AutoImage microscope. Spectra registration was performed in the wavelength range of 600–5000  $\text{cm}^{-1}$  with a spectral resolution of 2  $\text{cm}^{-1}$ . Apertures with the size of 50 and 75  $\mu\text{m}$  were used.

## 3. Results

When the resulting suspensions are kept for 5–10 days at 250  $^{\circ}\text{C}$ , the dark brown color of the initial Np(VI) lightens. This is more pronounced in the case of a dilute ammonia solution; in the saturated solution, the color change is insignificant. According to PXRD, the resulting products are poorly crystalline. Based on the data known for U(VI) phase formation under similar conditions, it can be assumed that the obtained precipitates are similar to schoepite [25], ammonium polyuranates [26] or framework U–O compound [27] and contain Np(VI) or Np(V). Increasing the dwell time at the indicated temperature does not lead to significant changes in a saturated ammonia solution, but in dilute ammonia small light green crystals were obtained as the only solid component of the reaction mixture after 45 days. A suitable crystal for X-ray structural analysis was selected from the precipitate.

### 3.1. X-ray Structure Analysis

Details of the single crystal X-ray experiment and main crystallographic data are given in Table 1; the principal bond lengths in the structure are listed in Table 2. Atomic coordinates are deposited at the Inorganic Crystal Structure Database, deposit number CSD 2215934.

The unit cell of  $(\text{NH}_4)[\text{NpO}_2\text{CO}_3]$  is shown in Figure 1. All atoms occupy special positions: Np1—position 2*d*, symmetry ( $-6m2$ ); O1—position 4*f*, symmetry ( $3m.$ ); C1—position 2*c*, symmetry ( $-6m2$ ); O2—position 6*h*, symmetry ( $mm2$ ); N1—position 2*a*, symmetry ( $-3m.$ ); H1A—position 4*e*, symmetry ( $3m.$ ); and H1B—position 12*k*, symmetry ( $.m.$ ). The H atoms are disordered by symmetry over two positions.

Each  $\text{NpO}_2$  group is surrounded by three carbonate anions; each anion by three  $\text{NpO}_2$  groups forming anionic layers (Figure 2). The layers with different orientations are stacked parallel to the (001) plane at  $z = \frac{3}{4}$  and  $z = \frac{1}{4}$ . Ammonium cations are placed between the anionic layers on *c* edges at  $z = \frac{1}{2}$ . The main features of the structure are in accordance with those described in earlier works [10–12] for  $\text{M}[\text{AnO}_2\text{CO}_3]$  compounds ( $\text{M} = \text{K}, (\text{NH}_4), \text{Rb}, \text{Cs}$ ).

**Table 1.** Crystal data and structure determination details for (NH<sub>4</sub>)[NpO<sub>2</sub>CO<sub>3</sub>].

|   |                                   |   |                |
|---|-----------------------------------|---|----------------|
| Empirical Formula                       | CH <sub>4</sub> NNpO <sub>5</sub> | $D_{\text{calc}}$ (g cm <sup>-3</sup> )                                   | 4.714          |
| Crystal size                            | 0.04 × 0.04 × 0.03 mm             | $\mu$ , mm <sup>-1</sup>  | 21.18          |
| $F_w$                                   | 374.05                            | Reflections collected   | 4630           |
| $T$ (K)                                 | 150 (2)                           | Independent reflections   | 165            |
| Crystal system                          | Hexagonal                         | Observed reflections [ $I > 2\sigma(I)$ ]                                 | 158            |
| Space group                             | $P6_3/mmc$                        | $R_{\text{int}}$  | 0.0559         |
| $a$ , (Å)                               | 5.0788 (6)                        | Number of parameters  | 19             |
| $c$ , (Å)                               | 10.9456 (19)                      | $R_1, wR_2$ [ $I > 2\sigma(I)$ ]  | 0.0102, 0.0234 |
| $V$ , (Å <sup>3</sup> )                 | 244.51 (7)                        | $R_1, wR_2$ [all data]  | 0.0114, 0.0237 |
| $Z$                                     | 2                                 | $GOOF$  | 1.203          |
| $D_{\text{calc}}$ (g cm <sup>-3</sup> ) | 4.714                             | $\Delta\rho_{\text{max}}, \Delta\rho_{\text{min}}$ , (e·Å <sup>-3</sup> ) | 0.687, -0.541  |

**Table 2.** Selected bond lengths ( $d$ , Å) in the structure of (NH<sub>4</sub>)[NpO<sub>2</sub>CO<sub>3</sub>].

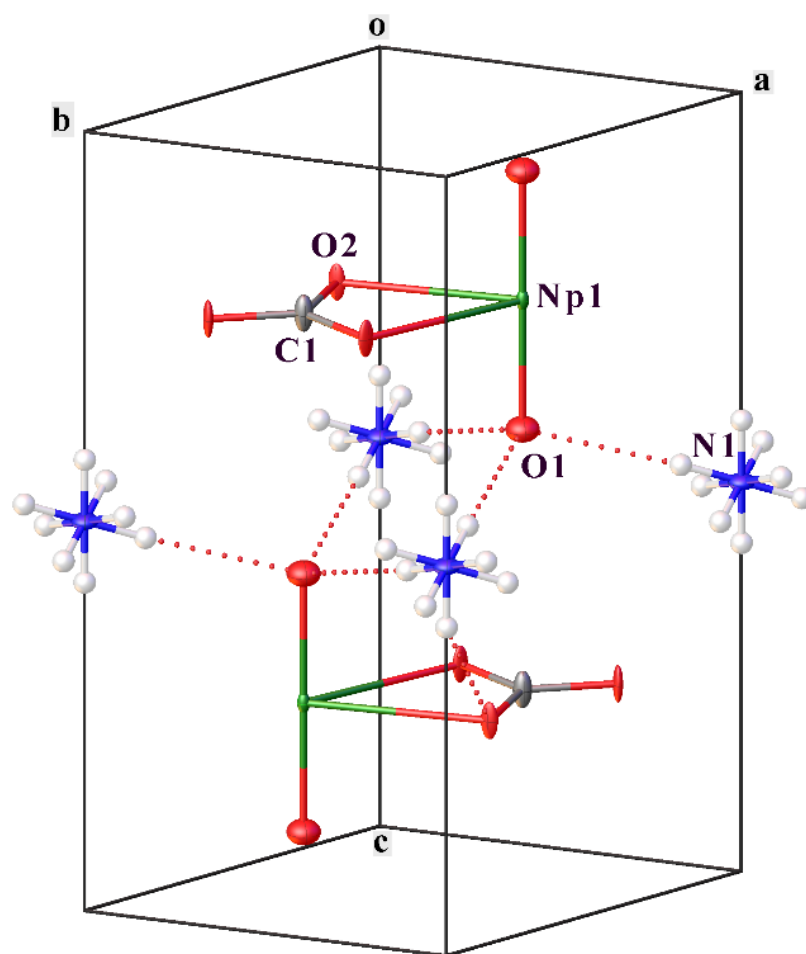
| Bond   | D              |
|--------|----------------|
| Np1-O1 | 2 × 1.815 (5)  |
| Np1-O2 | 6 × 2.5464 (4) |
| C1-O2  | 3 × 1.278 (3)  |
| N1-H1A | 0.86 (8)       |
| N1-H1B | 3 × 0.86 (8)   |

The coordination polyhedron of the Np atom is a hexagonal bipyramid. The Np-O distances (Table 2) are typical of Np(V). Hydrogen atoms of ammonium cations participate in H-bonds with O atoms of the NpO<sub>2</sub> group and carbonate anion. The H1A forms a “trifurcate” H-bond with N1 ... O2 distances of 3.1976(16) Å, the H1A ... O2 distances are 2.50(6) Å and N1-H1A ... O2 angles are 138.6(12)°. For the H-bonds N1-H1B ... O1 the N1 ... O1 distance is 3.0736(15) Å, the H1B distance is 2.21(8) Å and the angle N1-H1B ... O1 is 177(2)°.

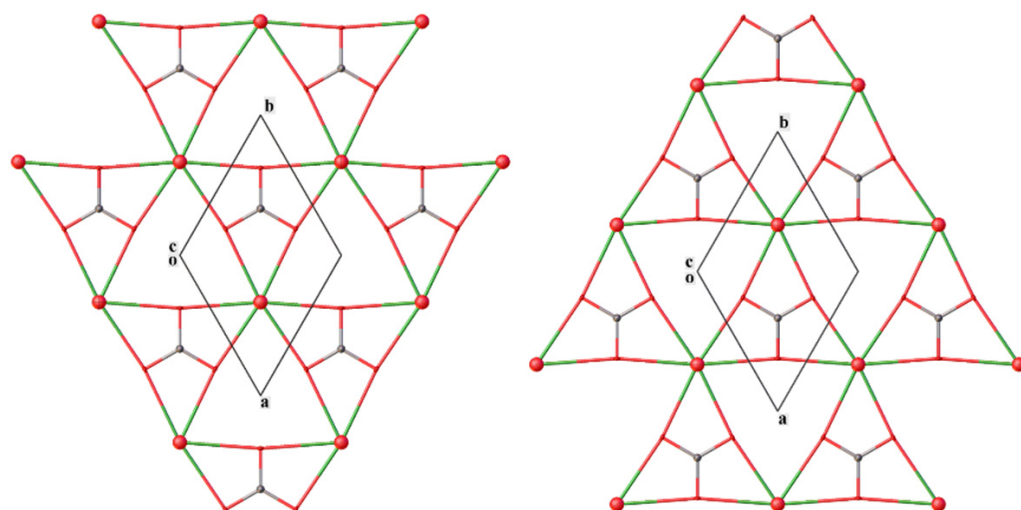
The PXRD data for the synthesized (NH<sub>4</sub>)[NpO<sub>2</sub>CO<sub>3</sub>] sample agree with the single crystal experiment (Figure S2), which indicates that the reaction product is a single phase. A comparison of cell parameters of isostructural M[AnO<sub>2</sub>CO<sub>3</sub>] compounds (Table 3) shows that the  $a$  constant (dimensions of anionic layers) is rather stable and the  $c$  constant (distance between anionic layers) varies significantly, mainly depending on the cation size. At the change of the temperature from 150 to 296 K, slow expansion of the anionic layers and reduction of the interlayer distance is observed.

### 3.2. X-ray Photoelectron Spectroscopy

The survey XPS spectrum of (NH<sub>4</sub>)[NpO<sub>2</sub>CO<sub>3</sub>] mainly shows (Figure 3A) neptunium, carbon and oxygen lines. The Np4f spectrum (Figure 3B) shows a spin-orbit doublet with the Np4f<sub>7/2</sub> binding energy of 402.9 eV and pronounced shake-up satellites shifted from the main lines by 9.4 eV. This shift is typical for Np(V) compounds [28]. The valence band spectrum (not shown) reveals a contribution from localized Np5f electrons near the Fermi edge, which also confirms the Np(V) oxidation state. A component in the C1s spectrum at a binding energy of 289.9 eV testifies to the presence of carbonate species [29]. The N1s line of NH<sub>4</sub><sup>+</sup> groups strongly overlaps with the intense Np4f<sub>7/2</sub> component, which precludes its reliable identification.



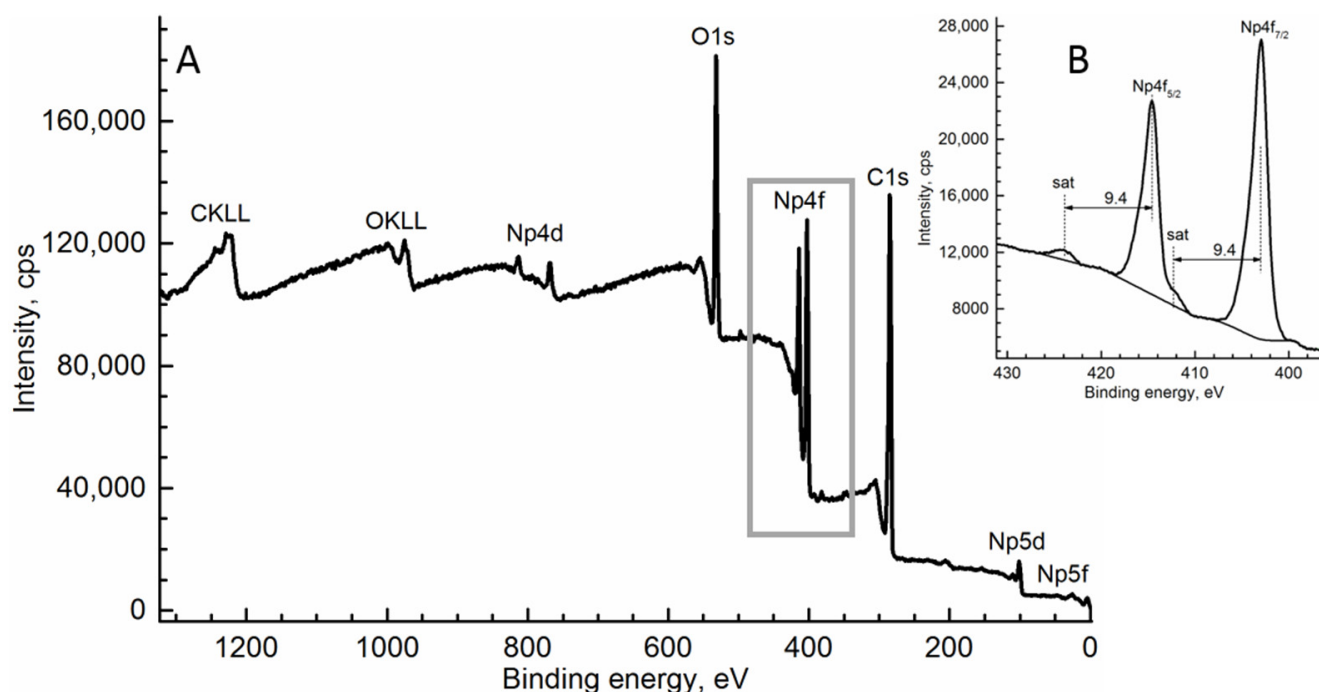
**Figure 1.** Unit cell of  $(\text{NH}_4)[\text{NpO}_2\text{CO}_3]$ . Temperature displacement ellipsoids are shown at 50% probability level. Dotted lines indicate H-bonds.



**Figure 2.** Anionic layers in the  $(\text{NH}_4)[\text{NpO}_2\text{CO}_3]$  structure. (Left):  $z = \frac{3}{4}$ , (Right):  $z = \frac{1}{4}$ .

**Table 3.** Unit cell parameters of  $M[\text{AnO}_2\text{CO}_3]$  compounds crystallizing in  $P6_3/mmc$  space group measured by powder X-ray diffraction.

| Compound                                 | a, Å        | c, Å          | Ref.      |
|--|-------------|---------------|-----------|
| $\text{K}[\text{NpO}_2\text{CO}_3]$      | 5.120 (1)   | 9.971 (3)     | [10]      |
| $\text{K}[\text{PuO}_2\text{CO}_3]$      | 5.093 (1)   | 9.815 (2)     | [10]      |
| $\text{K}[\text{PuO}_2\text{CO}_3]$      | 5.09 (1)    | 9.83 (2)      | [12]      |
| $\text{K}[\text{AmO}_2\text{CO}_3]$      | 5.112 (1)   | 9.740 (2)     | [10]      |
| $(\text{NH}_4)[\text{NpO}_2\text{CO}_3]$ | 5.09858 (4) | 10.89394 (14) | This work |
| $(\text{NH}_4)[\text{PuO}_2\text{CO}_3]$ | 5.09 (1)    | 10.39 (2)     | [12]      |
| $\text{Rb}[\text{AmO}_2\text{CO}_3]$     | 5.12 (1)    | 10.46 (4)     | [12]      |
| $\text{Cs}[\text{AmO}_2\text{CO}_3]$     | 5.123 (1)   | 11.538 (7)    | [11]      |

**Figure 3.** X-ray photoelectron spectra. (A)—Survey XPS spectrum; and (B)—Np4f spectrum of the  $(\text{NH}_4)[\text{NpO}_2\text{CO}_3]$ .

### 3.3. Vibrational Spectroscopy

The Raman spectrum of the  $(\text{NH}_4)[\text{NpO}_2\text{CO}_3]$  sample was compared with the spectrum of mixed U(VI)-ammonium carbonate  $(\text{NH}_4)_4[\text{UO}_2(\text{CO}_3)_3] \cdot 4\text{H}_2\text{O}$  synthesized according to the procedure described in [30]. As shown in Figure 4A, a similar set of spectral lines is observed for these compounds; this is consistent with related local structures. The Raman spectrum of  $(\text{NH}_4)[\text{NpO}_2\text{CO}_3]$  can be divided into three parts: low-frequency region up to  $200\text{ cm}^{-1}$ , containing bending vibrations of  $\text{NpO}_2^+$  and  $\text{CO}_3^{2-}$ ; stretching vibrations of the  $\text{NpO}_2^+$  cation at  $766\text{ cm}^{-1}$  [31,32], and peaks of  $\text{CO}_3^{2-}$  bending and stretching vibrations at  $718$  and  $1071\text{ cm}^{-1}$ , respectively [33]. The positions of the peaks of the carbonate group vibrations are consistent with those in ammonium uranyl carbonate and are within the characteristic range of the carbonate ion vibrations [34]. The position of the peak of symmetric stretching vibrations  $\nu_1(\text{NpO}_2^+)$  is shifted to lower frequencies relative to ammonium uranyl carbonate, which correlates with an increase in the  $\text{Np}=\text{O}$  bond length ( $1.82\text{ Å}$ ) in the neptunoyl fragment compared to the  $\text{U}=\text{O}$  length ( $1.79\text{ Å}$ ) in uranyl [35]. The absence of splitting of the  $\nu_3(\text{CO}_3^{2-})$  stretching peak additionally confirms the equivalence of all carbonate groups in the structure of the compound [36].

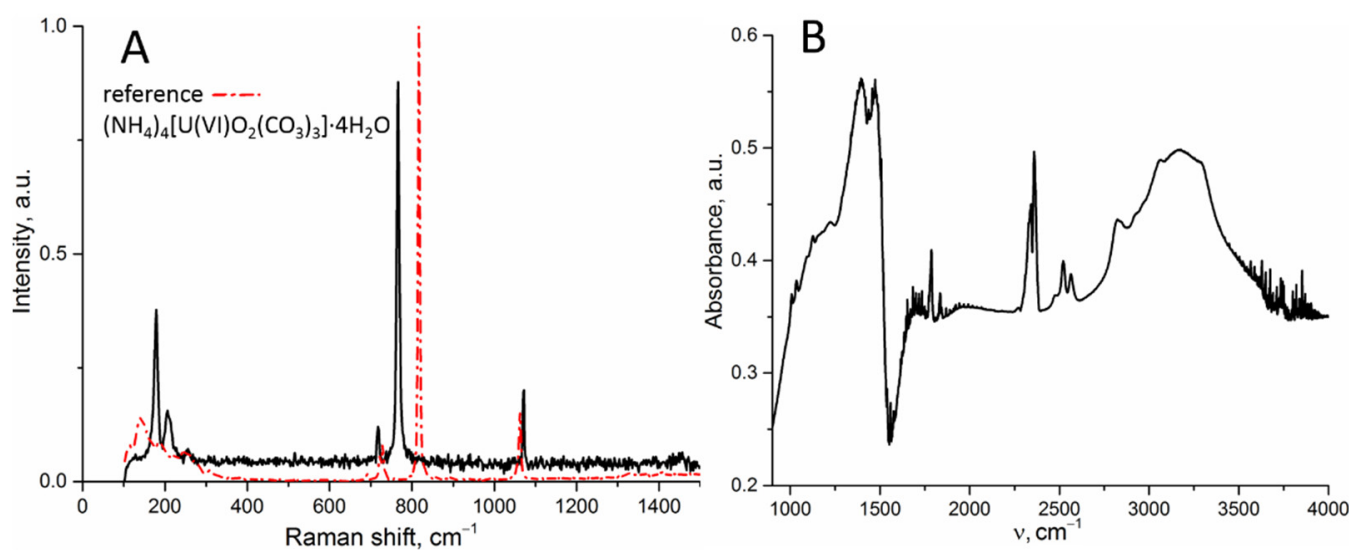


**Figure 4.** Spectroscopic data for the  $(\text{NH}_4)[\text{NpO}_2\text{CO}_3]$ . **(A)**—Raman spectra of the  $(\text{NH}_4)[\text{NpO}_2\text{CO}_3]$  (black line) and reference  $(\text{NH}_4)_4[\text{UO}_2(\text{CO}_3)_3]\cdot 4\text{H}_2\text{O}$  (red line) and **(B)**—IR absorption spectrum.

Due to the low intensity of the Raman lines corresponding to vibrations in  $\text{NH}_4^+$ , an infra-red absorption spectrum of  $(\text{NH}_4)[\text{NpO}_2\text{CO}_3]$  was recorded (Figure 4B). This spectrum contains peaks of N–H bond vibrations in  $\text{NH}_4^+$  at 1393 and 2900–3300  $\text{cm}^{-1}$  [37] as well as the peak of the carbonate anion at 1471  $\text{cm}^{-1}$ . The  $\text{CO}_3^{2-}$  vibrations overlap with the intense peak of the ammonium cation vibrations and contribute to the broadened shoulder at 1000–1200  $\text{cm}^{-1}$  [36,38]. Peaks at 2336 and 2360  $\text{cm}^{-1}$  are due to atmospheric  $\text{CO}_2$ .

#### 4. Discussion

The initial motivation for this work was an attempt to obtain Np(VI) compounds similar to those formed in the reaction of U(VI) with an ammonia solution. In [27], a framework compound  $(\text{NH}_4)_3(\text{H}_2\text{O})_2\{[(\text{UO}_2)_{10}\text{O}_{10}(\text{OH})][(\text{UO}_4)(\text{H}_2\text{O})_2]\}$  was made by hydrothermal synthesis at 220 °C. Despite the fact that the  $(\text{NH}_4)_2\text{CO}_3$  solution served as the source of ammonium cations, the formation of carbonates was not observed in the case of U(VI). In our case, the concentration of carbonate ions in the system was much lower, but carbonate complexes are the main reaction product. Thus, in contrast to U(VI), Np(V) carbonate complexes are much more stable under experimental conditions and their formation becomes preferable over oxyhydroxides. This result is quite unexpected and interesting in view of the fact that hydroxide complexes of f-elements are usually stronger than the carbonate complexes. This property is used, in particular, in the purification of actinides carbonate solutions by hydroxide precipitation. The possibility of the formation of uranium (V) carbonate complexes under similar conditions seems unlikely. Such compounds are present in solutions only, while reduction occurs as a result of electrolysis [17].

The reduction of Np(VI) in a solid state by hard-to-remove impurities, such as organic compounds in the presence of catalytic quantities of transition metals, is common in hydrothermal synthesis, e.g., at a temperature higher than 200 °C [39]. Probably, both the slow reduction of Np(VI) and low concentration of carbonate ions in the reaction mixture contributed to the formation of  $(\text{NH}_4)[\text{NpO}_2\text{CO}_3]$  crystals with sizes suitable for single crystal XRD. These considerations were confirmed by individual experiments on  $(\text{NH}_4)[\text{NpO}_2\text{CO}_3]$  synthesis, in which Np(V) in a carbonate-saturated ammonia solution was used as a precursor. The hydrothermal treatment of this mixture led to the formation of a grayish microcrystalline precipitate rather than large crystals.

Thus, in the course of the work,  $(\text{NH}_4)[\text{NpO}_2\text{CO}_3]$  single crystals were synthesized for the first time, which made it possible to accurately establish the structure of the compound.

It has been shown that neptunium (V) carbonate complexes are more stable with respect to hydroxide complexes in concentrated ammonium solution.

**Supplementary Materials:** The following supporting information can be downloaded at: <https://www.mdpi.com/article/10.3390/sym14122634/s1>, Figure S1: Design of the reactor used in the hydrothermal experiment; Figure S2: Le Bail fit of the PXRD data of the synthesized  $(\text{NH}_4)[\text{NpO}_2\text{CO}_3]$ .

**Author Contributions:** Conceptualization, V.G.P. and A.M.F.; methodology, V.G.P., I.M.N., M.S.G. and A.M.F.; validation, V.G.P., I.M.N., M.S.G. and A.M.F.; formal analysis, A.A.A., A.A.S., A.D.K., K.I.M. and Y.A.T.; investigation, A.A.A., A.A.S., A.D.K., K.I.M., Y.A.T. and I.M.N.; resources, V.G.P.; writing—original draft preparation, I.M.N. and M.S.G.; writing—review and editing, V.G.P., I.M.N., K.I.M., Y.A.T. and A.M.F.; visualization, V.G.P.; supervision, V.G.P., M.S.G. and A.M.F.; project administration, V.G.P., A.M.F.; funding acquisition, I.M.N. All authors have read and agreed to the published version of the manuscript.

**Funding:** This work was financially supported by the Russian Science Foundation, grant no. 21-73-00138.

**Data Availability Statement:** The data are available from the corresponding author on reasonable request.

**Acknowledgments:** XRD and vibrational spectroscopy measurements were performed using the equipment of the Center for Shared Use of IPCE RAS. As part of the XPS analysis, this work was supported by M.V. Lomonosov Moscow State University Program of Development.

**Conflicts of Interest:** The authors declare no conflict of interest.

## References

1. McKinley, I.G.; Russell Alexander, W.; Blaser, P.C. Development of Geological Disposal Concepts. In *Radioactivity in the Environment*; Elsevier: Amsterdam, The Netherlands, 2007; pp. 41–76.
2. Davis, J.A.; Kent, D.B. Surface Complexation Modeling in Aqueous Geochemistry. *Miner. Interface Geochem.* **1990**, *23*, 177–260.
3. Fernandes, M.M.; Scheinost, A.C.; Baeyens, B. Sorption of Trivalent Lanthanides and Actinides onto Montmorillonite: Macroscopic, Thermodynamic and Structural Evidence for Ternary Hydroxo and Carbonato Surface Complexes on Multiple Sorption Sites. *Water Res.* **2016**, *99*, 74–82. [[CrossRef](#)]
4. Romanchuk, A.Y.; Vlasova, I.E.; Kalmykov, S.N. Speciation of Uranium and Plutonium From Nuclear Legacy Sites to the Environment: A Mini Review. *Front. Chem.* **2020**, *8*, 630. [[CrossRef](#)] [[PubMed](#)]
5. Geckeis, H.; Lützenkirchen, J.; Polly, R.; Rabung, T.; Schmidt, M. Mineral-Water Interface Reactions of Actinides. *Chem. Rev.* **2013**, *113*, 1016–1062. [[CrossRef](#)] [[PubMed](#)]
6. Lopez, C.; Deschanel, X.; Bart, J.M.; Boubals, J.M.; Den Auwer, C.; Simoni, E. Solubility of Actinide Surrogates in Nuclear Glasses. *J. Nucl. Mater.* **2003**, *312*, 76–80. [[CrossRef](#)]
7. Sweet, L.E.; Corbey, J.F.; Gendron, F.; Autschbach, J.; McNamara, B.K.; Ziegelgruber, K.L.; Arrigo, L.M.; Peper, S.M.; Schwantes, J.M. Structure and Bonding Investigation of Plutonium Peroxocarbonate Complexes Using Cerium Surrogates and Electronic Structure Modeling. *Inorg. Chem.* **2017**, *56*, 791–801. [[CrossRef](#)]
8. Clark, D.L.; Hobart, D.E.; Neu, M.P. Actinide Carbonate Complexes and Their Importance in Actinide Environmental Chemistry. *Chem. Rev.* **1995**, *95*, 25–48. [[CrossRef](#)]
9. Pastoor, K.J.; Kemp, R.S.; Jensen, M.P.; Shafer, J.C. Progress in Uranium Chemistry: Driving Advances in Front-End Nuclear Fuel Cycle Forensics. *Inorg. Chem.* **2021**, *60*, 8347–8367. [[CrossRef](#)]
10. Keenan, T.K.; Kruse, F.H. Potassium Double Carbonates of Pentavalent Neptunium, Plutonium, and Americium. *Inorg. Chem.* **1964**, *3*, 1231–1232. [[CrossRef](#)]
11. Keenan, T.K. Lattice Constants of Some Alkali Metal Actinyl(V) Compounds. *Inorg. Chem.* **1965**, *4*, 1500–1501. [[CrossRef](#)]
12. Ellinger, F.H.; Zachariasen, W.H. The Crystal Structure of  $\text{KPuO}_2\text{CO}_3$ ,  $\text{NH}_4\text{PuO}_2\text{CO}_3$  and  $\text{RbAmO}_2\text{CO}_3$ . *J. Phys. Chem.* **1954**, *58*, 405–408. [[CrossRef](#)]
13. Burney, G.A. Separation of Americium from Curium by Precipitation of  $\text{K}_3\text{AmO}_2(\text{CO}_3)_2$ . *Nucl. Appl.* **1968**, *4*, 217–221. [[CrossRef](#)]
14. Choppin, G.R. Actinide Speciation in the Environment. *J. Radioanal. Nucl. Chem.* **2007**, *273*, 695–703. [[CrossRef](#)]
15. Kaszuba, J.P.; Runde, W.H. The Aqueous Geochemistry of Neptunium: Dynamic Control of Soluble Concentrations with Applications to Nuclear Waste Disposal. *Environ. Sci. Technol.* **1999**, *33*, 4427–4433. [[CrossRef](#)]
16. Ikeda-Ohno, A.; Tsushima, S.; Takao, K.; Rossberg, A.; Funke, H.; Scheinost, A.C.; Bernhard, G.; Yaita, T.; Hennig, C. Neptunium Carbonato Complexes in Aqueous Solution: An Electrochemical, Spectroscopic, and Quantum Chemical Study. *Inorg. Chem.* **2009**, *48*, 11779–11787. [[CrossRef](#)]
17. Ikeda, A.; Hennig, C.; Tsushima, S.; Takao, K.; Ikeda, Y.; Scheinost, A.C.; Bernhard, G. Comparative Study of Uranyl(VI) and -(V) Carbonato Complexes in an Aqueous Solution. *Inorg. Chem.* **2007**, *46*, 4212–4219. [[CrossRef](#)]

18. Vitova, T.; Pidchenko, I.; Schild, D.; Prüßmann, T.; Montoya, V.; Fellhauer, D.; Gaona, X.; Bohnert, E.; Rothe, J.; Baker, R.J.; et al. Competitive Reaction of Neptunium(V) and Uranium(VI) in Potassium–Sodium Carbonate-Rich Aqueous Media: Speciation Study with a Focus on High-Resolution X-Ray Spectroscopy. *Inorg. Chem.* **2020**, *59*, 8–22. [[CrossRef](#)]
19. Krause, L.; Herbst-Irmer, R.; Sheldrick, G.M.; Stalke, D. Comparison of Silver and Molybdenum Microfocus X-Ray Sources for Single-Crystal Structure Determination. *J. Appl. Crystallogr.* **2015**, *48*, 3–10. [[CrossRef](#)]
20. Sheldrick, G.M. A Short History of SHELX. *Acta Crystallogr. Sect. A Found. Crystallogr.* **2008**, *64*, 112–122. [[CrossRef](#)]
21. Sheldrick, G.M. SHELXT—Integrated Space-Group and Crystal-Structure Determination. *Acta Crystallogr. Sect. A Found. Adv.* **2015**, *71*, 3–8. [[CrossRef](#)]
22. Le Bail, A. Whole Powder Pattern Decomposition Methods and Applications: A Retrospection. *Powder Diffr.* **2005**, *20*, 316–326. [[CrossRef](#)]
23. Petříček, V.; Dušek, M.; Palatinus, L. Crystallographic Computing System JANA2006: General Features. *Zeitschrift Für Krist.-Cryst. Mater.* **2014**, *229*, 345–352. [[CrossRef](#)]
24. Vlasova, I.E.; Yapaskurt, V.O.; Averin, A.A.; Melnik, O.E.; Zolotov, D.A.; Senin, R.A.; Poliakova, T.R.; Nevolin, I.M.; Kalmykov, S.N.; Shiryaev, A.A. Nuclear Melt Glass from Experimental Field, Semipalatinsk Test Site. *Energies* **2022**, *15*, 9121. [[CrossRef](#)]
25. Finch, R.J.; Cooper, M.A.; Hawthorne, F.C.; Ewing, R.C. The Crystal Structure of Schoepite,  $[(\text{UO}_2)_8\text{O}_2(\text{OH})_{12}](\text{H}_2\text{O})_{12}$ . *Can. Mineral.* **1996**, *34*, 1071–1088.
26. Cordfunke, E.H.P. Composition and Structure of Ammonium Uranates. *J. Inorg. Nucl. Chem.* **1970**, *32*, 3129–3131. [[CrossRef](#)]
27. Li, Y.; Cahill, C.L.; Burns, P.C. Synthesis, Structural Characterization, and Topological Rearrangement of a Novel Open Framework U–O Material:  $(\text{NH}_4)_3(\text{H}_2\text{O})_2\{[(\text{UO}_2)_{10}\text{O}_{10}(\text{OH})][(\text{UO}_4)(\text{H}_2\text{O})_2]\}$ . *Chem. Mater.* **2001**, *13*, 4026–4031. [[CrossRef](#)]
28. Teterin, Y.A.; Teterin, A.Y. The Structure of X-Ray Photoelectron Spectra of Light Actinide Compounds. *Russ. Chem. Rev.* **2004**, *73*, 541–580. [[CrossRef](#)]
29. Shchukarev, A.; Korolkov, D. XPS Study of Group IA Carbonates. *Open Chem.* **2004**, *2*, 347–362. [[CrossRef](#)]
30. Zhang, L.; Zhou, J.; Zhang, J.; Su, J.; Zhang, S.; Chen, N.; Jia, Y.; Li, J.; Wang, Y.; Wang, J.-Q. Extraction of Local Coordination Structure in a Low-Concentration Uranyl System by XANES. *J. Synchrotron Radiat.* **2016**, *23*, 758–768. [[CrossRef](#)]
31. Basile, L.J.; Sullivan, J.C.; Ferraro, J.R.; LaBonville, P. The Raman Scattering of Uranyl and Transuranium V, VI, and VII Ions. *Appl. Spectrosc.* **1974**, *28*, 142–145. [[CrossRef](#)]
32. Fujii, T.; Uehara, A.; Kitatsuji, Y.; Yamana, H. Raman Spectroscopic Study on  $\text{NpO}_2^+ - \text{Ca}^{2+}$  Interaction in Highly Concentrated Calcium Chloride. *J. Radioanal. Nucl. Chem.* **2014**, *301*, 293–296. [[CrossRef](#)]
33. Krot, A.; Vlasova, I.; Trigub, A.; Averin, A.; Yapaskurt, V.; Kalmykov, S. From EXAFS of Reference Compounds to U(VI) Speciation in Contaminated Environments. *J. Synchrotron Radiat.* **2022**, *29*, 303–314. [[CrossRef](#)] [[PubMed](#)]
34. Tlili, M.M.; Amor, M.B.; Gabrielli, C.; Joiret, S.; Maurin, G.; Rousseau, P. Characterization of  $\text{CaCO}_3$  Hydrates by Micro-Raman Spectroscopy. *J. Raman Spectrosc.* **2002**, *33*, 10–16. [[CrossRef](#)]
35. Graziani, R.; Bombieri, G.; Forsellini, E. Crystal Structure of Tetra-Ammonium Uranyl Tricarbonate. *J. Chem. Soc. Dalt. Trans.* **1972**, *19*, 2059–2061. [[CrossRef](#)]
36. Frost, R.L.; Carmody, O.; Erickson, K.L.; Weier, M.L.; Čejka, J. Molecular Structure of the Uranyl Mineral Andersonite—A Raman Spectroscopic Study. *J. Mol. Struct.* **2004**, *703*, 47–54. [[CrossRef](#)]
37. Morgan, P.A.; Staats, H.W.; Goldstein, J.H. Infrared Spectra of  $\text{N}_{15}\text{H}_3$  and  $\text{N}_{15}\text{H}_4^+$ . *J. Chem. Phys.* **1957**, *27*, 4–6. [[CrossRef](#)]
38. Faulques, E.; Perry, D.L.; Kalashnyk, N. Vibrational Spectroscopy of a Crystallographically Unsettled Uranyl Carbonate: Structural Impact and Model. *Vib. Spectrosc.* **2018**, *99*, 184–189. [[CrossRef](#)]
39. Bessonov, A.A.; Afonasiyeva, T.V.; Krot, N.N. On Np (V) and (VI) formation at thermal decomposition of Np (IV) compounds. *Sov. Radiochem.* **1989**, *31*, 9–13.